

Provided for non-commercial research and education use.  
Not for reproduction, distribution or commercial use.



This article appeared in a journal published by Elsevier. The attached copy is furnished to the author for internal non-commercial research and education use, including for instruction at the authors institution and sharing with colleagues.

Other uses, including reproduction and distribution, or selling or licensing copies, or posting to personal, institutional or third party websites are prohibited.

In most cases authors are permitted to post their version of the article (e.g. in Word or Tex form) to their personal website or institutional repository. Authors requiring further information regarding Elsevier's archiving and manuscript policies are encouraged to visit:

<http://www.elsevier.com/copyright>



Contents lists available at ScienceDirect

## Computational Materials Science

journal homepage: [www.elsevier.com/locate/commatsci](http://www.elsevier.com/locate/commatsci)

## A new data reduction method for pulse diffusivity measurements on coated samples

Liguo Chen<sup>a</sup>, Andi M. Limarga<sup>b,\*</sup>, David R. Clarke<sup>b</sup><sup>a</sup> Global Engineering and Materials, Inc., Princeton, NJ 08540, United States<sup>b</sup> School of Engineering and Applied Sciences, Harvard University, Cambridge, MA 02138, United States

## ARTICLE INFO

## Article history:

Received 15 June 2010

Accepted 14 July 2010

Available online 5 August 2010

## Keywords:

Thermal diffusivity

Coated sample

Numerical method

## ABSTRACT

A new method, based on numerical solutions of the heat conduction equation, is presented for reducing flash diffusivity data to determine the diffusivity of a coating on a substrate of known thermal properties. Measurements are performed with a conventional thermal flash apparatus and the calculated curve from the numerical simulations is fitted to the measured temperature–time curve, the “thermogram”. The current work is a natural extension of previous work on single layer, homogeneous samples [1]. The main advantage of this new data reduction method, which incorporates nonlinear least-squares regression, is that both the thermal diffusivity of the coating and the thermal contact resistance can be determined. When the thermal contact resistance is small, the solution automatically converges to the perfect thermal contact case. To demonstrate its efficacy, the method is first implemented by analyzing a group of simulated data and then applied to a set of experimental data obtained from three different bilayer samples.

© 2010 Elsevier B.V. All rights reserved.

## 1. Introduction

The use of layered composites and coatings in a number of applications such as thermal barriers, emissivity control, electrical insulation and wear, and erosion or corrosion resistance protection has rapidly increased in recent years. In many of these materials systems, the thermal diffusivity is an important parameter but can also be different than the notional value of the pure coating material because of the manner in which it is applied. For instance, the thermal performance of thermal barrier coatings, which are used to provide thermal insulation to metallic components in gas turbine engines, depends on the microstructure and porosity of the coating, which are characteristics of the coating deposition process [2]. Coatings of the same yttria-stabilized zirconia composition deposited by plasma-spraying and electron-beam deposition (EB-PVD) can have very different diffusivities because of their very different distribution and shape of the porosity entrained during the deposition process [3]. Furthermore, measurement of a free-standing thermal barrier coating to conduct single layer sample measurement is usually not possible because of the fragility of the coating and the difficulty in removing large areas of the coating. Currently, the thermal diffusivities of coatings are usually determined by applying the thermal flash technique [4] to a coated substrate and applying a model to derive the diffusivity using the known properties of the substrate [5,6]. There are, however, intrinsic difficulties associated with the determination of the coating diffusivity and interface resistance, that this paper addresses.

Models for determining the diffusivity rely on theories for thermal conduction in layered materials with varying interface resistances. One theory was presented by Lee and Taylor [7,8] who proposed a data reduction method for determining the thermal diffusivity based on the use of  $t_{1/2}$  point in the measured plot of rear-surface temperature versus time graph – the “thermogram” – recorded following a thermal pulse applied to the front surface. This measurement is based on the findings of the original analysis for homogeneous samples by Parker et al. [4], where  $t_{1/2}$  is the time needed to reach half of the maximum temperature following a thermal pulse. Sweet [9] extended Lee’s analysis to include both thermal losses at the boundaries and a thermal contact resistance between the layers. A quadrupole formalism of the Laplace transformation technique described by Degiovanni [10] also takes into account heat losses. By considering the sensitivity coefficients for a number of cases, Koski [11] gave a detailed analysis of how the errors in the measurement of additional properties can propagate through the data reduction and result in inaccuracies in the thermal diffusivity.

Although these existing data reduction methods have been quite successful and are codified in the software of several commercial thermal flash systems, they rely on knowing the thermal contact resistance at the interface or assuming it is zero. In reality, the thermal contact resistance value is usually unknown or difficult to measure, and the values can be very different from sample to sample even though they are made from same materials. Large errors in the derived thermal diffusivity can be produced if the thermal contact resistance value is not known accurately. One objective of the current work is to introduce a data reduction method for determining the thermal diffusivity of the coating

\* Corresponding author. Tel.: +1 617 496 4295.

E-mail address: [limarga@seas.harvard.edu](mailto:limarga@seas.harvard.edu) (A.M. Limarga).

material without knowing the thermal contact resistance *a priori*. The proposed data reduction method uses a nonlinear parameter estimation technique based on numerical solutions of the heat conduction equation [1]. We will also show using an averaging approach that the thermal diffusivity and thermal contact resistance can be successfully decoupled and both calculated with a reasonable accuracy.

## 2. Theoretical model

The formulae needed for the data reduction procedure can be derived as solutions of the heat conduction equation, along with initial and boundary conditions corresponding to the selected model. The model assumes one-dimensional heat flow through a two-layered sample with uniform and constant thermophysical properties of both layers. The front face is uniformly subjected to the instantaneous heat pulse with the heat  $Q$  supplied to the unit area (Fig. 1). The thicknesses of the first and the second layer are  $L_1$  and  $L_2$ , respectively with a total thickness  $L = L_1 + L_2$ . The transient temperature rise in the sample can be obtained by solving the heat conduction equation for each layer:

$$\frac{\partial T_1}{\partial t} = \alpha_1 \frac{\partial^2 T_1}{\partial x^2} \quad (0 \leq x \leq L_1, t > 0) \quad (1)$$

$$\frac{\partial T_2}{\partial t} = \alpha_2 \frac{\partial^2 T_2}{\partial x^2} \quad (L_1 \leq x \leq L_2, t > 0) \quad (2)$$

where  $t$  is time,  $\alpha$  is thermal diffusivity, subscripts “1” and “2” denote the first layer and second layer, respectively.  $x$  is the space coordinate and  $T = T(x, t)$  is the temperature rise produced by the thermal flash at the space–time point  $(x, t)$ . Thus, the initial condition (before the heat pulse) can be written as follows:

$$T(x, 0) = 0 \quad (3)$$

Considering the heat loss to the environment, the boundary condition at the front face is:

$$-k_1 \frac{\partial T_1}{\partial x} \Big|_{x=0} = Q\delta(0) - h_1 T_1(0, t) \quad (4)$$

where  $\delta(0)$  is the Dirac delta function for the flash pulse [12] and  $h$  is the coefficient of heat transfer from the surface of the sample to its surroundings. Typically, the Biot number ( $Bi_i = h_i L_i / k_i$ ) is used as a parameter to characterize the heat loss [13].  $k$  is the thermal conductivity and can be related to thermal diffusivity as  $k = \rho C \alpha$ , where  $\rho$  is the density and  $C$  is specific heat. Assuming continuous heat flux across the interface, the boundary condition at the interface can be expressed as follows:

$$-k_1 \frac{\partial T_1}{\partial x} \Big|_{x=L_1} = \frac{T_2(L_1, t) - T_1(L_1, t)}{R} = -k_2 \frac{\partial T_2}{\partial x} \Big|_{x=L_1} \quad (5)$$

where  $R$  is the thermal contact resistance. Lastly, assuming that the heat flux at the back face is equal to the heat loss, the boundary condition at the back face can be written as:

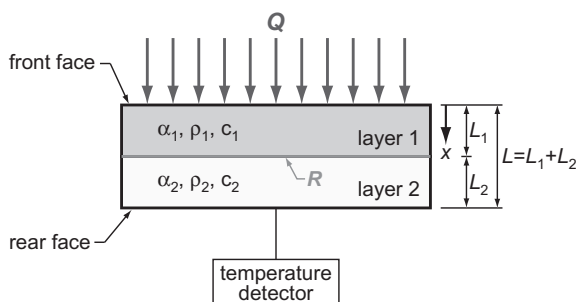


Fig. 1. Schematic diagram of the thermal flash method and the coating geometry.

$$-k_2 \frac{\partial T_2}{\partial x} \Big|_{x=L_2} = h_2 T_2(L, t) \quad (6)$$

## 3. Numerical method

Numerical implementation of Eqs. (1)–(6) requires the time  $t$  to be discretized into small time steps  $\Delta t$  and the two-layers discretized into  $N_1$  and  $N_2$  volume elements of thickness  $\Delta x$  along the heat flow direction. For the first layer, Eq. (1) can be rewritten as:

$$\frac{T(x, t + \Delta t) - T(x, t)}{\Delta t} = \alpha_1 \frac{T(x + \Delta x, t) - 2T(x, t) + T(x - \Delta x, t)}{\Delta x^2} \quad (7)$$

and for the second layer, Eq. (2) becomes:

$$\frac{T(x, t + \Delta t) - T(x, t)}{\Delta t} = \alpha_2 \frac{T(x + \Delta x, t) - 2T(x, t) + T(x - \Delta x, t)}{\Delta x^2} \quad (8)$$

At the boundaries in Eqs. (7) and (8), the terms  $T(-\Delta x, t)$  and  $T(L + \Delta x, t)$  are eliminated using the boundary conditions at the front and back surfaces (Eqs. (4) and (6)):

$$\frac{T(\Delta x, t) - T(-\Delta x, t)}{2\Delta x} = -\frac{Q}{k_1} \delta(t) - \frac{h_1}{k_1} T(0, t) \quad (9)$$

$$\frac{T(L + \Delta x, t) - T(L - \Delta x, t)}{2\Delta x} = -\frac{h_2}{k_2} T(L, t) \quad (10)$$

At the interface between the coating and the substrate,  $T_1(L_1, t)$  and  $T_2(L_1, t)$  denote the interfacial temperature of layers 1 and 2, respectively. Eq. (5) can be discretized using the “ghost fluid” technique [14]:

$$-k_1 \frac{T_1(L_1, t) - T_1(L_1 - 0.5\Delta x, t)}{0.5\Delta x} = \frac{T_2(L_1, t) - T_1(L_1, t)}{R} \quad (11)$$

$$-k_2 \frac{T_2(L_1 + 0.5\Delta x, t) - T_2(L_1, t)}{0.5\Delta x} = \frac{T_2(L_1, t) - T_1(L_1, t)}{R} \quad (12)$$

In order to maintain numerical stability, the time step  $\Delta t$  and the grid size  $\Delta x$  are related by the von Neuman relationship [15]:

$$\Delta t \leq \frac{0.5\Delta x^2}{\max(\alpha_1, \alpha_2)} \quad (13)$$

The numerical method was tested by implementing it to a simple problem with known analytical solutions. Assuming perfect thermal contact between the layers and neglecting the heat loss effect ( $h = 0$ ), the rear-surface temperature of the layered sample is given by the solution at  $x = L_2$  as follows [7]:

$$T(t) = T_m \left[ 1 + 2 \sum_{k=1}^{\infty} \frac{(\omega_1 \chi_1 + \omega_2 \chi_2) e^{-(\gamma_k/\eta_2)^2 t}}{\omega_1 \chi_1 \cos(\gamma_k \omega_1) + \omega_2 \chi_2 \cos(\gamma_k \omega_2)} \right] \quad (14)$$

where

$$\chi_1 = \Lambda_{1/2} + 1, \quad \chi_2 = \Lambda_{1/2} - 1, \quad \omega_1 = \eta_{1/2} + 1, \quad \omega_2 = \eta_{1/2} - 1 \quad (15)$$

$$\Lambda_i = \sqrt{\rho_i c_i k_i}, \quad \eta_i = L_i / \sqrt{\alpha_i} \quad (16)$$

$$\Lambda_{1/2} = \Lambda_1 / \Lambda_2, \quad \eta_{1/2} = \eta_1 / \eta_2 \quad (17)$$

and  $\gamma_k$  is the  $k$ th positive root of the characteristic equation of

$$\chi_1 \sin(\gamma \omega_1) + \chi_2 \sin(\gamma \omega_2) = 0 \quad (18)$$

$T_m$  is the steady state temperature in the sample after the pulse given by

$$T_m = \frac{Q}{\rho_1 c_1 L_1 + \rho_2 c_2 L_2} \quad (19)$$

By comparing our numerical calculations with the analytical solution, our studies show that using a grid with  $N_1 = N_2 = 20$  is sufficient to converge to the analytical solution and thereby verify numerical method code.

#### 4. Parameter estimation

The parameter estimation approach to data reduction involves determining the parameters of interest through a least square curve fitting of the calculated model to experimentally obtained data. The fitting is performed by minimizing the mean square error between the measured temperature versus time data and, in our case, that predicted from numerical solutions. The parameters of interest serve as the variables for the curve fitting process. Advantages of the method include the following:

- (i) Reduction of noise distortions to the transient signal. This is particularly important when the data includes significant noise that prevents simple application of more standard techniques.
- (ii) Low quality data and irregularities can be readily identified by comparing the experimental data and the calculated curve. This makes it possible to reject poor quality data sets allowing only high quality experimental data to be used. In turn, more accurate results can be obtained.

To apply the parameter estimation method, the following parameters need to be known: the physical density, specific heat, thermal diffusivity and the thickness of the substrate as well as the density, specific heat and the thickness of the coating. The heat loss coefficients are normally small and are found to be not very sensitive to the solution, so we assume that the heat loss coefficients for the front face and for the back face have the same value. This assumption leaves four unknown parameters: the thermal diffusivity of the coating, the thermal contact resistance, the heat transfer coefficient or Biot number for the surfaces, as well as the laser pulse energy absorbed by the sample or the steady state temperature. The effects of these parameters have to be determined by the parameter estimation process.

##### 4.1. Sensitivity coefficients

As part of the process of obtaining a nonlinear least-squares curve fit of the calculated solutions to the experimental data, the sensitivity coefficient [16]

$$S_i = P_i \frac{\partial \tilde{T}}{\partial P_i} \quad (20)$$

must be derived.  $S_i$  are the sensitivity coefficients,  $\tilde{T}$  is the normalized temperature rise and  $P_i$  are the curve fit parameters. Formally,  $S_i$  is the fractional change in temperature by a unit fractional change in  $P_i$ . The sensitivity coefficients indicate the relative importance of the fit parameters. Essentially,  $S_i$  is the change in the fitted curve produced by changing individual parameters, and reflects the accuracy of that parameter extracted by the estimation method. In general, large sensitivity coefficients are desired, particularly for those parameters of interest (the thermal diffusivity in our case). Sensitivity coefficients of unknown parameters for a simulated run from the numerical solution are shown in Fig. 2. The input parameters were typical of those for thermal barrier coatings,  $\alpha_1 = 0.01 \text{ cm}^2/\text{s}$ ,  $L_1 = 0.1 \text{ cm}$ ,  $\rho_1 C_1 = 10 \text{ J/cm}^3 \text{ K}$ ,  $R = 0.25 \text{ cm}^2 \text{ K/W}$ ,  $\alpha_2 = 0.02 \text{ cm}^2/\text{s}$ ,  $L_2 = 0.1 \text{ cm}$ ,  $\rho_2 C_2 = 20 \text{ J/cm}^3 \text{ K}$  and  $Bi = 0.01$ . The figure illustrates several features:

- (i) The magnitude of the sensitivity coefficient for diffusivity is larger than of the other parameters. It is most sensitive around the half time,  $t_{1/2}$  – the time at which the rear-face temperature rise reaches one half of its maximum value. This means that we have to include most of the thermogram in the least square curve fitting to obtain an accurate estimation.

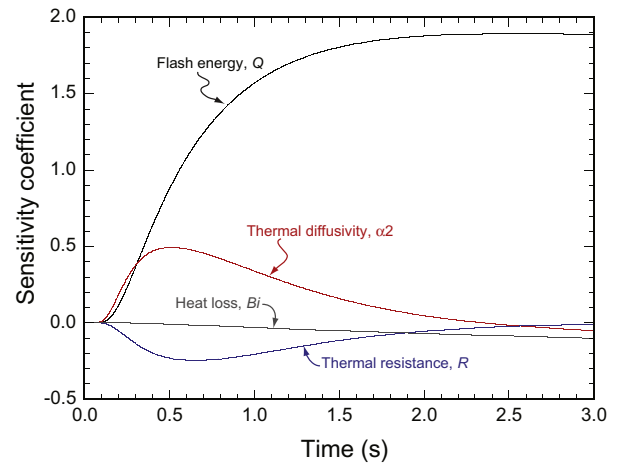


Fig. 2. Sensitivity coefficients of the unknown parameters for a simulated run. The input parameters were  $\alpha_1 = 0.01 \text{ cm}^2/\text{s}$ ,  $L_1 = 0.1 \text{ cm}$ ,  $\rho_1 C_1 = 10 \text{ J/cm}^3 \text{ K}$ ,  $R = 0.25 \text{ cm}^2 \text{ K/W}$ ,  $\alpha_2 = 0.02 \text{ cm}^2/\text{s}$ ,  $L_2 = 0.1 \text{ cm}$ ,  $\rho_2 C_2 = 20 \text{ J/cm}^3 \text{ K}$  and  $Bi = 0.01$ . These values are typical of those used to evaluate thermal barrier coatings.

- (ii) The solution is not very sensitive to the heat loss parameter  $Bi$  but it is sensitive to the absorbed flash energy, particularly at longer times.
- (iii) The thermal contact resistance has obviously smaller sensitivity compared to the thermal diffusivity, but it is much larger than the heat loss parameter. It also reaches its maximum at around half time and goes to zero at longer times.

In summary, the sensitivity analysis and parameter estimation process show that an accurate determination can be expected for the thermal diffusivity and absorbed flash energy and the steady state temperature. However, less accurate results can be expected for the estimation of the thermal contact resistance and the heat loss parameter. As will be shown later the estimation of the thermal contact resistance can be further improved by making, and analyzing, a series of repeated measurements under the same experimental conditions.

##### 4.2. Implementation on simulated data

To check the accuracy of our data reduction method, we first implemented it on sets of simulated data as shown in Fig. 3. This simulated data set was generated using Eqs. (7)–(13) with the addition of Gaussian noise and treated as an experimental thermogram. Our data reduction method was then applied to calculate the thermal diffusivity. This approach allows us to evaluate the accuracy of the data reduction method since the value of thermal diffusivity was used in generating the simulated data set. The input parameters for generating the raw data in Fig. 3 were the same as used in Fig. 2:  $\alpha_1 = 0.01 \text{ cm}^2/\text{s}$ ,  $L_1 = 0.1 \text{ cm}$ ,  $\rho_1 C_1 = 10 \text{ J/cm}^3 \text{ K}$ ,  $R = 0.25 \text{ cm}^2 \text{ K/W}$ ,  $T_m = 2 \text{ K}$ ,  $\alpha_2 = 0.02 \text{ cm}^2/\text{s}$ ,  $L_2 = 0.1 \text{ cm}$ ,  $\rho_2 C_2 = 20 \text{ J/cm}^3 \text{ K}$  and  $Bi = 0.01$ . The standard deviation of the noise was 2.5% of  $T_m$ . In the parameter estimation process, the initial values of  $\alpha_2$ ,  $R$ ,  $Bi$  and  $T_m$  are given, and the iteration was carried out until the convergence condition was met.

The calculated temperature rise from the numerical method is shown in Fig. 3 and compared to the simulated raw data. The calculated results were  $T_m = 2.01 \text{ K}$ ,  $\alpha_2 = 2.10 \times 10^{-2} \text{ cm}^2/\text{s}$ ,  $R = 0.27 \text{ cm}^2 \text{ K/W}$  and  $Bi = 9.30 \times 10^{-3}$ . The errors in the calculated values for  $\alpha_2$  and  $R$  (5% and 4%, respectively) are relatively large because of the linear dependency of the thermal gradient across the interface on the product  $\alpha_2 R$ , and similar shape of their sensi-

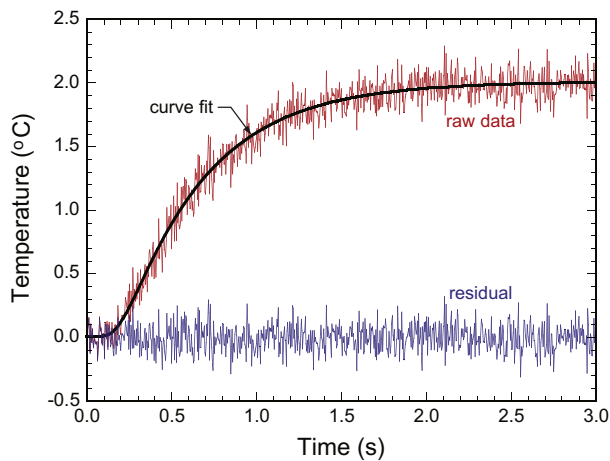


Fig. 3. Example of a curve fitting result to a simulated raw data thermogram together with the fitting residuals.

tivity coefficients (Fig. 2). In the literature it has been concluded that the thermal diffusivity and thermal contact resistance cannot both be obtained simultaneously because of this linear dependency [9,11,17]. For this reason either a value for the thermal contact resistance based on experience is commonly used to calculate thermal diffusivity or it is assumed it is zero. We consider another approach as described in the following paragraph.

In the simulated experimental data, the noise was randomly generated so that different simulation results were obtained when the parameter estimation was applied to different simulation sets. So, we ran 20 sets of tests for the same group of input parameters and calculated the thermal diffusivity and the thermal contact resistance for each set of data. The ratio of calculated parameter values to the input real values are determined and plotted in Figs. 4 and 5. For comparison, the average of the twenty simulations was calculated. It is apparent that as a result of the random nature of the noise, the simulated values of the diffusivity and thermal resistance also have some scatter. The values deviate from the input value by as much as 15% for both the thermal diffusivity and thermal contact resistance. However, the average value of the thermal diffusivity only has an error of 0.13% and the thermal contact resistance has an error of 2.54%. Despite the scatter from individual runs, most data are clustered within 5% of the real value for the thermal diffusivity. This is similar to the accuracy of thermal flash measurements made on homogeneous materials [18]. Consistent

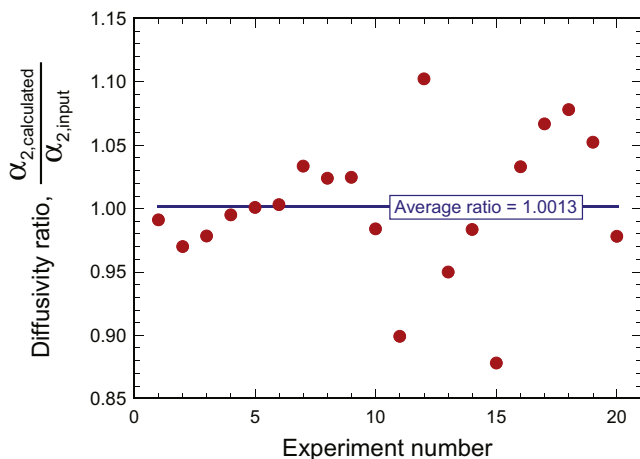


Fig. 4. Ratio of the calculated diffusivity values to the input diffusivity for 20 sets of simulation runs.

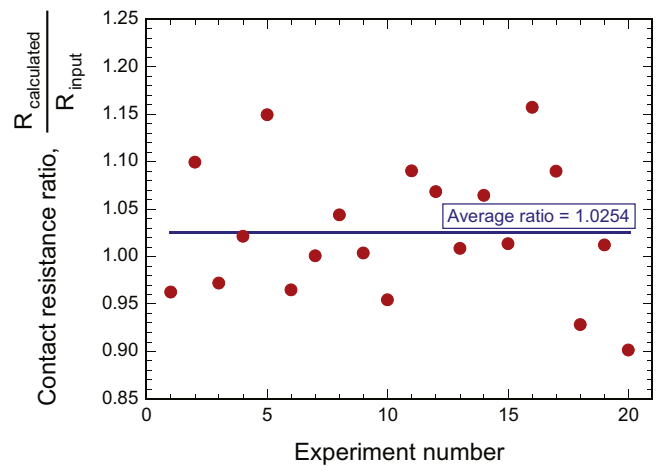


Fig. 5. Ratio of calculated thermal contact resistance value to the input value for 20 sets of simulation runs.

with the sensitivity coefficient analysis, the thermal interface resistance  $R$ , was determined less accurately, mostly clustered within 10% of the real value. The calculated average and standard deviation are also shown in Table 1.

#### 4.3. Error propagation

It is important to note that the determination of thermal diffusivity of one layer in a layered sample is a dependent measurement, meaning that the estimation of the thermal diffusivity of one layer and the thermal contact resistance requires the knowledge of the other properties. Errors in the measurement of the additional properties are propagated through the data reduction and result in calculation inaccuracies of thermal diffusivity. This is illustrated in Fig. 6 that shows the error of the diffusivity  $\alpha_2$  caused by errors of input parameters namely  $\rho_1 C_1$ ,  $\rho_2 C_2$ ,  $\alpha_1$ ,  $L_1$  and  $L_2$ . In each case, the errors caused are almost linearly dependent on the input parameter errors. It is worth noting that the uncertainty in the thickness of the layers has the largest effect on the measurement error in thermal diffusivity. Therefore, precise measurement of the thicknesses is critical to determining the thermal diffusivity with any accuracy.

### 5. Implementation on experimental data

In order to demonstrate the use of this data reduction method in flash thermal diffusivity measurement, we present the results made on three different two-layer samples, two formed by bonding together metal disks of known thermal properties and the other a thermal barrier coating deposited on a superalloy and provided by its manufacturer, Howmet Corporation.

#### 5.1. Experimental apparatus and sample preparation

Thermal diffusivity measurements were performed using Flash-line 3000 instrument (Anter Corp., Pittsburgh, PA). This instrument

Table 1  
Comparison between the input values used to generate simulated experimental data and the calculated fitting results average of 20 sets of data.

Parameter	$\alpha_2$ (cm <sup>2</sup> /s)	$T_m$ (K)	$R$ (cm <sup>2</sup> K/W)	$Bi$
Input value	0.02	2.00	0.25	$10 \times 10^{-3}$
Calculated average	0.02	2.01	0.26	$9.40 \times 10^{-3}$
Standard deviation	$1.10 \times 10^{-3}$	$9.50 \times 10^{-3}$	$6.97 \times 10^{-2}$	$4.0 \times 10^{-4}$
Error	0.13%	0.64%	2.56%	6.00%

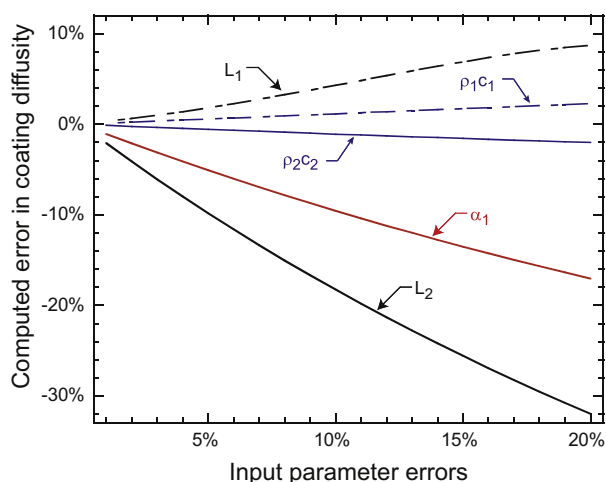


Fig. 6. Computed errors in determining the diffusivity  $\alpha_2$  caused by errors in the input physical parameters shown.

uses a xenon flash lamp under computer control to impart a brief but controlled amount of energy to the sample. The light travels through a quartz light pipe, which ensures that the entire front side surface of the sample is uniformly heated. A similar light pipe on the back side of the sample is connected to an In–Sb thermal radiation detector, cooled with liquid nitrogen, to measure the temperature of the back surface of two-layer samples.

Three different samples were used to evaluate the data reduction method described in this study. The first sample was prepared by bonding aluminum and copper disks (12.7-mm diameter, 3-mm thickness) with colloidal silver as an interlayer. The excess silver was driven out by clamping the disks together, followed by a thermal treatment at 150 °C for 30 min to promote curing of the silver interlayer. The second sample was prepared by bonding an aluminum disk (12.7-mm diameter, 3-mm thickness) to a stainless steel disk with similar diameter (1-mm thickness) using indium bonding. The third sample was a 7 wt.% yttria-stabilized zirconia (7YSZ) thermal barrier coating deposited on a thin nickel-based superalloys via electron-beam physical vapor deposition (EB-PVD) method (Howmet Corporation, Whitehall, MI). Following standard practice, a thin carbon coating (approximately 10  $\mu\text{m}$  thick) was then applied to both sides of the specimens to improve the absorption of the heat pulse at the front face and have the same emissivity of the back face.

The physical properties of the materials used are listed in Table 2. The thermal diffusivities of each metal disk were measured by single layer thermal flash experiment [19], except for the TBC as the free-standing coating was not available. The values were then used in the measurements of the two-layer samples to

Table 2  
Material properties of the materials used in this study.

Specimen number	Material	Density (g/cm <sup>3</sup> )	Heat capacity (J/g K)	Diffusivity (cm <sup>2</sup> /s)	Thickness (mm)
I	Copper	8.94	0.396	1.20	2.98
	Aluminum	2.71	0.933	Treated as unknown	3.01
II	Aluminum	2.71	0.933	0.78	3.00
	Stainless steel	7.91	0.508	Treated as unknown	1.00
III	Superalloy	8.92	0.415	$2.50 \times 10^{-2}$	0.37
	EB-PVD	4.49	0.509	Treated as unknown	0.16
	TBC				

calculate the diffusivity of the disk that was treated as the unknown. The density and heat capacity of the individual disks were evaluated by the Archimedes method and Differential Scanning Calorimetry, respectively. The experimental thermogram obtained from test samples was analyzed using our data reduction method to calculate the thermal diffusivity of the material representing the coating. The material properties and sample thicknesses shown in Table 2 were used as inputs in the curve fitting algorithm.

The thermal diffusivity of one layer was calculated using the data reduction method introduced in last sections by treating it as a fitting parameter while the other properties listed in Table 2 were held constant. The calculated thermal diffusivity of aluminum and stainless steel from this two-layer sample measurement was then compared to that obtained from a single layer sample measurement.

### 5.2. Experimental results

Fig. 7 shows the measured thermogram for the copper/aluminum test sample at 100 °C, normalized by the maximum temperature rise. The experimental data has been smoothed using a high frequency noise filter, but there are still large fluctuations due to low frequency noise that is rather difficult to remove [20]. Also plotted on the same figure is the calculated fitted curve using the parameter estimation method. The random distribution of the residuals suggests that the fitted curve agrees well with the experimental curve. Similar to the treatment of the numerically generated data described earlier in Section 4.2, we performed multiple test runs on the same sample (30 independent tests) to obtain both the average thermal diffusivity of the aluminum layer in the aluminum/copper bilayered sample and the average thermal contact resistance at the interface. The results were then compared to the thermal diffusivity of the aluminum obtained from a single layer aluminum specimen (Table 3). The same procedure was applied to the aluminum/stainless steel sample with the stainless steel layer as the unknown and the results were listed in Table 4. In both cases, the discrepancy between thermal diffusivity of the layer of interest in the bilayer sample and that measured as a homogeneous single layer was about 5%. The thermal contact resistances of the copper/aluminum and aluminum/stainless steel bilayers were found to be high, 0.28 and 2.39 cm<sup>2</sup> K/W, respectively. Unfortunately, verification of the thermal contact resistances could not be made as we have no method of independently measuring this parameter. Furthermore, it can be expected that as the interface has a small but finite thickness as

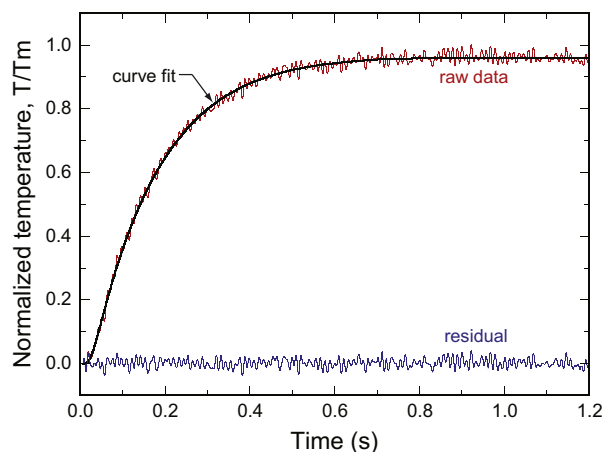


Fig. 7. An example of the curve fitting to an experimental thermogram measured on a copper/aluminum test bilayer together with the fitting residuals.

**Table 3**

Comparison between the aluminum properties measured in the bilayer (copper/aluminum) sample and a single disk of aluminum.

	Thermal diffusivity (cm <sup>2</sup> /s)	Thermal contact resistance (cm <sup>2</sup> K/W)
Measurement of aluminum in a bilayer	0.82 ± 0.21	0.28 ± 0.02
Measurement of aluminum disk	0.78 ± 0.01	NA
Error	5.10%	NA
Textbook value [28]	0.84	NA

**Table 4**

Comparison between stainless steel properties determined from a bilayer (aluminum/stainless steel) sample and a single disk of stainless steel.

	Thermal diffusivity (cm <sup>2</sup> /s)	Thermal contact resistance (cm <sup>2</sup> K/W)
From measurement of the bilayer	$4.42 \times 10^{-2} \pm 6.2 \times 10^{-3}$	2.39 ± 0.16
Measurement of stainless steel disk	$4.22 \times 10^{-2} \pm 2.0 \times 10^{-4}$	NA
Error	4.74%	NA
Textbook value [28]	$4.00 \times 10^{-2}$	NA

a result of the bonding process used to make the model bilayer, no unique or reference values exists, and that the high thermal resistance is a result of an interfacial layer being formed between the two-layers.

The thermal diffusivity of the thermal barrier coating deposited on the nickel-based superalloy substrate was found to be  $9.9 \times 10^{-3}$  cm<sup>2</sup>/s and the thermal contact resistance was found to be  $3.3 \times 10^{-3}$  cm<sup>2</sup> K/W. Measurement on a single layer, free-standing TBC was not possible but the measured diffusivity is consistent with other thermal flash measurements of similar zirconia coatings prepared by electron-beam deposition and reported in the literature [21]. It is also consistent with the limited number of results obtained using two other *in situ* diffusivity methods, one based on laser-induced luminescence and infrared radiometry [22] and the other based on the “phase of photothermal measurements” [23]. The latter technique, which evaluates the phase lag between a modulated CO<sub>2</sub> laser heating the coating and the thermal emission from the coating, gave a thermal diffusivity of  $1.00 \times 10^{-2}$  cm<sup>2</sup>/s when applied to the same coating sample as evaluated in this paper. It was also reported that the interfacial thermal contact resistance between the thermal barrier coating deposited on a metallic substrate was  $3.47 \times 10^{-3}$  cm<sup>2</sup> K/W [24], consistent with the value obtained in this study. It is worth noting that the thermal contact resistance derived in this study is not inconsistent with the values obtained from incoherent interfaces between very dissimilar materials formed during growth, for instance  $6 \times 10^{-4}$  cm<sup>2</sup> K/W for the diamond/corderite interface [25]. It is emphasized that the thermal contact resistance was evaluated for the coating in its as-deposited condition prior to high-temperature aging. After high-temperature aging in air, for instance over many hours at 1150 °C, oxidation occurs at the interface forming an intermediate oxide layer of a few microns and local delaminations at the TBC/metal interface can also develop [26]. Concurrently the diffusivity of the coating changes as the microstructure and porosity evolve [27]. Because both the diffusivity and thermal resistance change, the data reduction method de-

scribed in this work is well suited to quantify both of these effects as will be described in a later communication.

## 6. Concluding remarks

A new data reduction method for reducing flash diffusivity data obtained on coatings is described. This method is based on numerical solutions of the heat conduction equation and uses a nonlinear parameter estimation technique. The main advantage of this method is that the thermal diffusivity of the coating can be determined without knowing *a priori* the thermal contact resistance. The parameter estimation results are sensitive to the random errors introduced during the experiment, so that multiple measurements are required in order to filter out the effect of statistical noise. Another advantage is that the interface thermal resistance can also be obtained from repeated measurements using the data reduction method. The data reduction method was evaluated on sets of simulated data, followed by its implementation on a set of experimental data obtained from three different bilayer samples bonded in different ways. The thermal diffusivity results obtained are consistent with other diffusivity measurements and the thermal contact resistances are considered to be reasonable.

## References

- [1] L.G. Chen, D.R. Clarke, *Computational Materials Science* 45 (2009) 342.
- [2] D.R. Clarke, C.G. Levi, *Annual Review of Materials Research* 33 (2003) 383.
- [3] J.R. Nicholls, K.J. Lawson, A. Johnstone, D.S. Rickerby, *Surface and Coatings Technology* 151–152 (2002) 383.
- [4] W.J. Parker, R.J. Jenkins, C.P. Butler, G.L. Abbott, *Journal of Applied Physics* 32 (1961) 1679.
- [5] K.B. Larson, K. Koyama, *Journal of Applied Physics* 39 (1968) 4408.
- [6] W. Hohenauer, L. Vozar, *High Temperatures – High Pressures* 33 (2001) 297.
- [7] H.J. Lee, *Thermal Diffusivity in Layered and Dispersed Composites*, Ph.D. Thesis, West Lafayette: Purdue University, 1975.
- [8] H.J. Lee, R.E. Taylor, *Journal of Applied Physics* 47 (1976) 148.
- [9] J.N. Sweet, *Thermal Conductivity* 20 (1989) 287.
- [10] A. Degiovanni, *International Journal of Heat and Mass Transfer* 31 (1988) 553.
- [11] J.A. Koski, Improved data reduction method for laser pulse diffusivity determination with the use of minicomputers, in: *Proceedings of the 8th Symposium on Thermophysical Properties*, vol. 2, The American Society of Mechanical Engineers, New York, 1981, p. 94.
- [12] J. Gembarovic, R.E. Taylor, *International Journal of Thermophysics* 14 (1993) 297.
- [13] W.M. Deen, *Analysis of Transport Phenomena*, Oxford University Press, New York, 1998.
- [14] F. Gibou, L.G. Chen, D. Nguyen, S. Banerjee, *Journal of Computational Physics* 222 (2007) 536.
- [15] J.H. Ferziger, M. Peric, *Computational Methods for Fluid Dynamics*, Springer, New York, 2002.
- [16] R.C. Beck, K.J. Arnold, *Parameter Estimation in Engineering and Science*, John Wiley and Sons, New York, 1977.
- [17] G. Wei, X. Zhang, F. Yu, K. Chen, *International Journal of Thermophysics* 27 (2006) 235.
- [18] Y. Tan, J.P. Longtin, S. Sampath, H. Wang, *Journal of the American Ceramic Society* 92 (2009) 710.
- [19] L. Vozar, W. Hohenauer, *High Temperatures – High Pressures* 35–36 (2003) 253.
- [20] L. Pawlowski, P. Fauchais, C. Martin, *Revue de Physique Appliquée* 20 (1985) 1.
- [21] H.J. Ratzler-Scheibe, U. Schulz, *Surface and Coatings Technology* 201 (2007) 7880.
- [22] B. Heeg, D.R. Clarke, *Journal of Applied Physics* 104 (2008) 113119.
- [23] T.D. Bennett, F.L. Yu, *Journal of Applied Physics* 97 (2005) 013520.
- [24] F. Yu, T.D. Bennett, *Journal of Applied Physics* 98 (2005) 103501.
- [25] C.-W. Nan, R. Birringer, D.R. Clarke, H. Gleiter, *Journal of Applied Physics* 81 (1997) 6692.
- [26] V.K. Tolpygo, D.R. Clarke, K.S. Murphy, *Surface and Coatings Technology* 188–189 (2004) 62.
- [27] T.R. Kakuda, A.M. Limarga, T.D. Bennett, D.R. Clarke, *Acta Materialia* 57 (2009) 2583.
- [28] F.P. Incropera, D.P. DeWitt, *Fundamentals of Heat and Mass Transfer*, John Wiley & Sons, Inc., New York, 2002.